Calibration of the temporally varying volatility and interest rate functions

Eunchae Park, Jisang Lyu, Sangkwon Kim, Chaeyoung Lee, Wonjin Lee, Yongho Choi, Soobin Kwak, Changwoo Yoo, Hyeongseok Hwang & Junseok Kim

ARTICLE

Check for updates

Calibration of the temporally varying volatility and interest rate functions

Eunchae Park[a], Jisang Lyu[a], Sangkwon Kim[a], Chaeyoung Lee[a], Wonjin Lee[b], Yongho Choi[c], Soobin Kwak[a], Changwoo Yoo[b], Hyeongseok Hwang[b] and Junseok Kim [a]

[a]Department of Mathematics, Korea University, Seoul, Republic of Korea; [b]Department of Financial Engineering, Korea University, Seoul Republic of Korea; [c]Department of Mathematics and Big Data, Daegu University, Gyeongsan-si, Gyeongsangbuk-do, Republic of Korea

ABSTRACT

In this study, we develop a calibration method of the temporally varying volatility and interest rate functions using the Black–Scholes (BS) partial differential equation and the observed market option prices with different strikes and expiries. The proposed method uses the piecewise linear interpolations between data points which are defined at the middle points of maturity dates. When we construct the volatility and interest rate, we use the exponential function so that the interpolated values are always positive. Numerical experiments with synthetic and real market data demonstrate the superior performance of the proposed method.

1. Introduction

The main purpose of this paper is to develop a calibration algorithm of the time-dependent volatility and interest rate functions using the Black–Scholes (BS) equation. In [18], the authors studied a transformation of the equation with time-varying parameters to provide a more general approach. The observed market option prices with different strikes and expiries:

$$\frac{\partial u(S,t)}{\partial t} + \frac{1}{2}[\sigma(t)S]^2 \frac{\partial^2 u(S,t)}{\partial S^2} + r(t)S\frac{\partial u(S,t)}{\partial S} - r(t)u(S,t) = 0, \tag{1}$$

for $(S,t) \in \mathbb{R}^+ \times [0,T]$, where $u(S,t)$ is the option value of the underlying price S and time t. Here, $\sigma(t)$ and $r(t)$ are the time-dependent volatility and interest rate functions of time t, respectively. The final condition is the payoff function $u(S,T) = \Lambda(S)$ at expiry T.

In 1973, Black and Scholes [2] derived the BS equation with constant volatility and interest rate. This model is one of the most widely used models in the option pricing field. However, the constant parameter does not reflect arbitrage-free market and volatility skew, etc. To solve this problem, many researchers presented different methods for time-dependent parameters. Elettra and Rossella [5] derived the Geske formula for compound options with time-dependent volatility and interest rate and compared them with the Geman–El Karoui–Rochet formula. Yunxia and Xiping [23] considered the underlying asset driven by the Ornstein–Uhlenback (OU) process and the interest rates driven by the Hull–White model in order to price the European call and put options. The OU process does not make any economic assumptions in the actuarial approach, hence it applies not only

---

CONTACT Junseok Kim ✉ cfdkim@korea.ac.kr 📧 Department of Mathematics, Korea University, Seoul 02841, Republic of Korea

to the arbitrage-free, equilibrium, and complete markets but also to arbitrage, non-equilibrium, and incomplete markets. Guardasoni [8] straightforwardly applied semi-analytical method for pricing of barrier options with time-dependent interest rate, volatility, and dividend. It may be considered as an alternative approach for the BS equation with time-dependent parameters. In [11], a solution of an ordinary differential equation in which the time-dependent interest rate is assumed to be zero in standard deviation of the interest rate from the Vasicek model is applied to the BS equation. In addition, there are various studies related to the time-dependent volatility and interest rate using BS equation [14,16–19].

There are also many authors who studied the reconstruction of local volatility using the stochastic volatility model [10], which was developed to overcome the disadvantage of the BS model. In [7], the authors investigated the Heston hybrid model with a stochastic interest rate, which combines a stochastic volatility equity and interest rate process, and presented the approximations for the model by emphasizing the importance of speed of pricing. When their model is used, there is no need for several calculations. Grzelak [6] proposed a new local volatility framework which allows large-stepping simulation. He and Chen [9] developed a closed-form solution for the European call options using stochastic volatility models. In [1], a stochastic local volatility technique was introduced for valuating exotic options by finite difference method. In [13], a closed-form formula was presented to aid the calibration of the regime-switching model to resolve the time-intensive problems. Daněk and Pospíšil also developed another regime-switching algorithm for the stochastic volatility jump diffusion model [4]. In [12], the authors presented a method to price derivatives with stochastic volatility and stochastic interest rate through the conditional Monte Carlo framework. Until now, nevertheless, the BS equation continued to be used and studied steadily as mentioned above. In this study, we present the method for calibration of the time-dependent volatility and interest rate functions using the BS equation.

The rest of the paper is organized as follows. In Section 2, we explain our numerical algorithm for constructing the time-dependent volatility function and interest rate function. In Section 3, computational tests are described. Conclusions are made in Section 4.

2. Numerical algorithm

Let S be the underlying asset price and $\tau = T - t$ be the time to expiry. Then, Equation (1) can be rewritten as

$$\frac{\partial u(S, \tau)}{\partial \tau} = \frac{1}{2}[\sigma(\tau)S]^2 \frac{\partial^2 u(S, \tau)}{\partial S^2} + r(\tau)S\frac{\partial u(S, \tau)}{\partial S} - r(\tau)u(S, \tau), \tag{2}$$

for $(S, \tau) \in \Omega \times (0, T]$ with $u(S, 0) = \Lambda(S)$ for $S \in \Omega = (0, L)$ [20]. We numerically solve Equation (2) using a finite difference method (FDM). Let $u_i^n \equiv u(S_i, n\Delta\tau)$ be the numerical approximation of the solution of Equation (2) for $i = 1, 2, \ldots, N_S$ and $n = 0, 1, \ldots, N_\tau$. Here, $\Delta\tau = T/N_\tau$ is uniform temporal step size and N_τ is the number of time steps. We use the non-uniform asset price domain. Figure 1 shows the non-uniform grid. Here, we define the spatial step size $h_{i-1} = S_i - S_{i-1}$.

Let $\sigma^n \equiv \sigma(n\Delta\tau)$ and $r^n \equiv r(n\Delta\tau)$ be the discrete variable volatility and interest rate, respectively. By applying the fully implicit-in-time and non-uniform space difference scheme to Equation (2), we
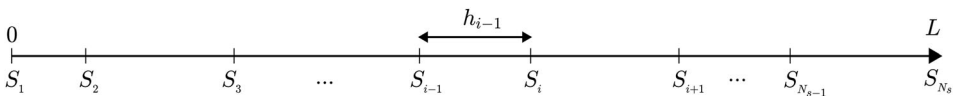

Figure 1. Non-uniform grid with a spatial step size h_{i-1}.

obtain that

$$\frac{u_i^{n+1} - u_i^n}{\Delta \tau} = \frac{(\sigma^{n+1} S_i)^2}{2} \left(\frac{2u_{i-1}^{n+1}}{h_{i-1}(h_{i-1} + h_i)} - \frac{2u_i^{n+1}}{h_{i-1}h_i} + \frac{2u_{i+1}^{n+1}}{h_i(h_{i-1} + h_i)} \right)$$

$$+ r^{n+1} S_i \left(\frac{-h_i u_{i-1}^{n+1}}{h_{i-1}(h_{i-1} + h_i)} + \frac{(h_i - h_{i-1})u_i^{n+1}}{h_{i-1}h_i} + \frac{h_{i-1}u_{i+1}^{n+1}}{h_i(h_{i-1} + h_i)} \right)$$

$$- r^{n+1} u_i^{n+1}. \tag{3}$$

We can rewrite the above Equation (3) as

$$\alpha_i u_{i-1}^{n+1} + \beta_i u_i^{n+1} + \gamma_i u_{i+1}^{n+1} = b_i, \quad \text{for } i = 2, \ldots, N_S, \tag{4}$$

where $\alpha_i = \frac{r^{n+1} S_i h_i}{h_{i-1}(h_{i-1}+h_i)} - \frac{(\sigma^{n+1} S_i)^2}{h_{i-1}(h_{i-1}+h_i)}$, $\beta_i = \frac{1}{\Delta \tau} - \frac{r^{n+1} S_i(h_i-h_{i-1})}{h_{i-1}h_i} + \frac{(\sigma^{n+1} S_i)^2}{h_{i-1}h_i} + r^{n+1}$, $\gamma_i = -\frac{r^{n+1} S_i h_{i-1}}{h_i(h_{i-1}+h_i)} - \frac{(\sigma^{n+1} S_i)^2}{h_i(h_{i-1}+h_i)}$, and $b_i = \frac{u_i^n}{\Delta \tau}$. For boundary conditions, we use the zero Dirichlet condition at S_1, that is, $u_1^{n+1} = 0$ and the linear condition at S_{N_S}, that is, $u_{N_S+1}^{n+1} = 2u_{N_S}^{n+1} - u_{N_S-1}^{n+1}$ for all n [22]. To solve the resulting discrete tri-diagonal system (4), we apply the Thomas algorithm [21].

Next, we present the proposed algorithm for constructing the temporally varying volatility and interest rate using option prices. Suppose that we have a set of measurements $\{U_\beta^\alpha\}$, where U_β^α is the market price of the options with the exercise time T_α for $\alpha = 1, \ldots, M_t$ and the exercise price K_β for $\beta = 1, \ldots, M_k$. Here, we assume that $T_1 < \ldots < T_{M_t}$ and $K_1 < \cdots < K_{M_k}$. Using the given data, we determine a piecewise volatility function $\sigma(t)$ and a piecewise interest rate function $r(t)$ in the least-squares sense. That is, we minimize the following mean-square error (MSE):

$$\mathcal{E}(\sigma, r) = \frac{1}{M_t M_k} \sum_{\alpha=1}^{M_t} \sum_{\beta=1}^{M_k} \omega_\beta^\alpha [u_{K_\beta}(\sigma, r; S_0, T_\alpha) - U_\beta^\alpha]^2, \tag{5}$$

where $u_{K_\beta}(\sigma, r; S_0, T_\alpha)$ is the numerical solution at $S = S_0$ of Equation (2) with the strike price K_β at time T_α. Here, ω_β^α is a normalized weight, i.e. trading volume of U_β^α. Let W_β^α be the trading volume of U_β^α, then we define the normalized weight as $\omega_\beta^\alpha = W_\beta^\alpha / \sum_{\gamma=1}^{M_k} W_\gamma^\alpha$, which implies $\sum_{\gamma=1}^{M_k} \omega_\beta^\alpha = 1$ for $\alpha = 1, \ldots, M_t$.

In this study, we use the *lsqcurvefit* routine, which is a non-linear curve-fitting solver in MATLAB R2019a [15], to find the optimal values σ and r that minimize the cost function $\mathcal{E}(\sigma, r)$. Now, we present the detailed process of the proposed algorithm. We use the notation $T_{\alpha+\frac{1}{2}} = (T_\alpha + T_{\alpha+1})/2$ for $\alpha = 1, \ldots, M_t - 2$.

Given initial guess $\tilde{\sigma}_\alpha^0$ ($\alpha = 1, \ldots, M_t$), we define the piecewise linear volatility function as

$$\sigma(t) = \begin{cases} \frac{\sigma_2^0 - \sigma_1^0}{T_{\frac{3}{2}}} t + \sigma_1^0, & \text{if } t \in [0, T_{\frac{3}{2}}], \\[2mm] \frac{\sigma_{\alpha+1}^0 - \sigma_\alpha^0}{T_{\alpha+\frac{1}{2}} - T_{\alpha-\frac{1}{2}}} (t - T_{\alpha-\frac{1}{2}}) + \sigma_\alpha^0, & \text{if } t \in [T_{\alpha-\frac{1}{2}}, T_{\alpha+\frac{1}{2}}], \; 2 \le \alpha \le M_t - 2, \\[2mm] \frac{\sigma_{M_t}^0 - \sigma_{M_t-1}^0}{T_{M_t} - T_{M_t-\frac{3}{2}}} (t - T_{M_t-\frac{3}{2}}) + \sigma_{M_t-1}^0, & \text{if } t \in [T_{M_t-\frac{3}{2}}, T_{M_t}], \end{cases}$$
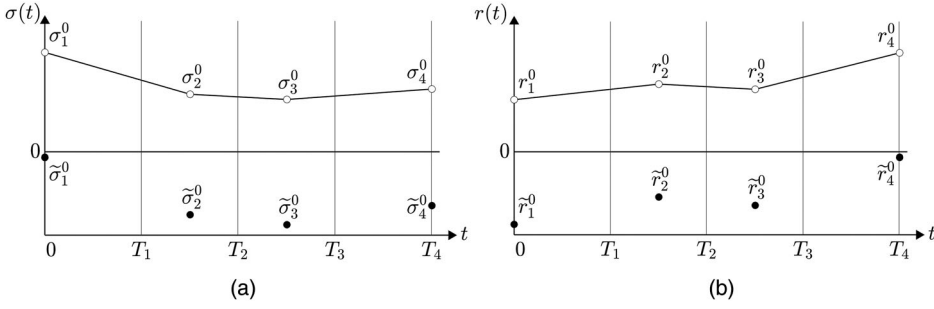
Figure 2. Schematic illustrations of the piecewise linear (a) volatility function and (b) interest rate function from our proposal.

where $\sigma_\alpha^0 = \exp(\tilde{\sigma}_\alpha^0)$. Similarly, given initial guess $\tilde{r}_\alpha^0$ ($\alpha = 1, \ldots, M_t$), the piecewise linear interest rate function is defined as

$$
r(t) = \begin{cases}
\frac{r_2^0 - r_1^0}{T_{\frac{3}{2}}} t + r_1^0, \text{ if } t \in [0, T_{\frac{3}{2}}], \\[2mm]
\frac{r_{\alpha+1}^0 - r_\alpha^0}{T_{\alpha+\frac{1}{2}} - T_{\alpha-\frac{1}{2}}} (t - T_{\alpha-\frac{1}{2}}) + r_\alpha^0, \text{ if } t \in [T_{\alpha-\frac{1}{2}}, T_{\alpha+\frac{1}{2}}], \ 2 \le \alpha \le M_t - 2, \\[2mm]
\frac{r_{M_t}^0 - r_{M_t-1}^0}{T_{M_t} - T_{M_t-\frac{3}{2}}} (t - T_{M_t-\frac{3}{2}}) + r_{M_t-1}^0, \text{ if } t \in [T_{M_t-\frac{3}{2}}, T_{M_t}],
\end{cases}
$$

where $r_\alpha^0 = \exp(\tilde{r}_\alpha^0)$. Note that we can avoid the negative value in $\sigma(t)$ and $r(t)$ by using the exponential function. Figure 2 illustrates the piecewise linear volatility and interest rate functions, respectively. The black dots mean the initial guess points and the white dots mean the value that substituted the initial guess points using the exponential function. We can obtain initial piecewise linear functions by interpolating these points.

Using these initial volatility and interest rate functions, we start the *lsqcurvefit* routine to find the optimal values σ and r that minimize the cost function $\mathcal{E}(\sigma, r)$.

3. Computational tests

Now, we show the performance of the proposed time-dependent volatility construction algorithm by computational tests with manufactured volatility functions, interest rate function and option data from a real market. All computations are performed on a 3.60 GHz Intel PC with 8 GB of RAM loaded with MATLAB R2019a. If there is no other mention, we use the uniform temporal step size $\Delta\tau = 1/360$ and the non-uniform spatial grid $\Omega = \{15i \mid i = 0, \ldots, 5\} \cup \{80 + 1.25j \mid j = 0, \ldots, 32\} \cup \{125 + 15k \mid k = 0, \ldots, 11\}$ in the following experiments. Additionally, we assume the prices are equally weighted, that is, the trading volumes of each strike with the same maturity are the same.

3.1. Manufactured data 1

First, we consider the following non-linear manufactured volatility and interest rate functions:

$$
\sigma(t) = 0.3e^{-t}, \quad r(t) = 0.5t^2 + 0.1. \tag{6}
$$

Next, we obtain reference values for the call option that are based on these manufactured volatility function and interest rate function (6) by solving Equation (3) with $T_\alpha = 90\alpha/360$ for $\alpha = 1, 2, 3, 4$ and $K_\beta = 70 + 10\beta$ for $\beta = 1, 2, \ldots, 5$. The European call option prices generated by the given functions (6) are represented in Table 1.

Table 1. European call option prices generated by the volatility and interest rate functions $\sigma(t) = 0.3e^{-t}$, $r(t) = 0.5t^2 + 0.1$.

K_β	80	90	100	110	120
$T_1 = 90/360$	22.96	13.63	6.02	1.80	0.36
$T_2 = 180/360$	25.86	17.12	9.78	4.73	1.93
$T_3 = 270/360$	28.66	20.34	13.17	7.72	4.11
$T_4 = 360/360$	31.34	23.37	16.35	10.70	6.56
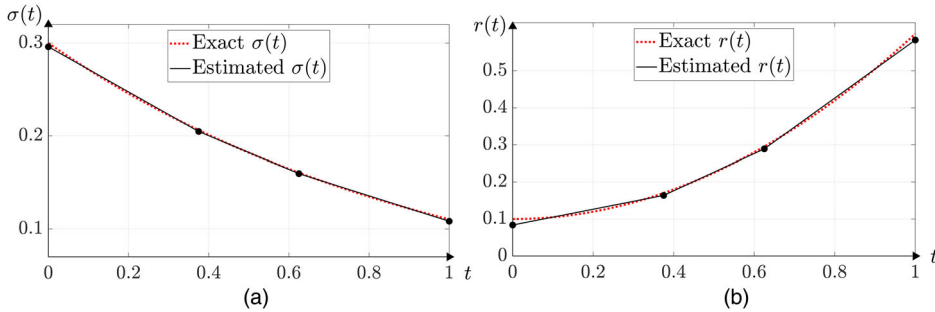
Figure 3. Estimated piecewise linear functions from the proposed algorithm compared to (a) the exact volatility function $\sigma(t) = 0.3e^{-t}$ and (b) the exact interest rate function $r(t) = 0.5t^2 + 0.1$.
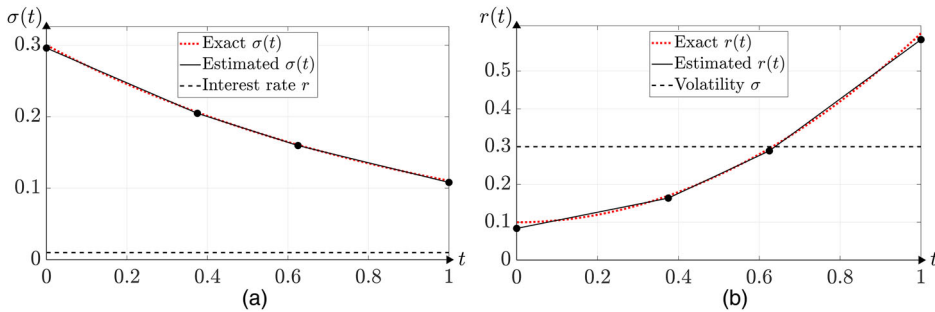
Figure 4. Estimated piecewise linear functions from the proposed algorithm compared to (a) the exact volatility function $\sigma(t) = 0.3e^{-t}$, with fixed interest rate $r = 0.01$ and (b) the exact interest rate function $r(t) = 0.5t^2 + 0.1$, with fixed volatility $\sigma = 0.3$.

Then, we demonstrate the proposed algorithm with the initial guesses $\tilde{\sigma}_n^0 = -2$, $\tilde{r}_n^0 = -2$, $n = 1, 2, 3, 4$. Figure 3 illustrates the obtained piecewise linear volatility and interest rate functions. Here, we denote the exact functions with the dotted line and the estimated functions from our algorithm with the solid line. Also, we have inserted the point set $\{\sigma_n, r_n\}$, $n = 1, 2, 3, 4$ with some dots on the black solid line. From these figures, we can confirm our proposed method satisfactorily recovers the exact volatility and interest rate functions. We present the MSE between the estimated functions from the numerical test and the exact ones. The values are 1.1413e-6 and 2.9398e-5 for volatility and interest rate, respectively.

At this time, we conduct tests by fixing one of two variables to be constant. Figure 4 represents the results obtained. Figure 4(a) indicates the volatility function obtained when the interest rate $r = 0.01$ is fixed and Figure 4(b) indicates the volatility function obtained when the volatility $\sigma = 0.3$ is fixed. As shown in Figure 3, we use the same mark representations. Furthermore, we add the constant interest rate and the constant volatility in the two graphs. Even if each interest rate or volatility is fixed as a constant, a satisfactory result could be confirmed.

Next, we consider this test without taking exponentiation when we calibrate. Given initial guess $\sigma_\alpha^0, r_\alpha^0 (\alpha = 1, \ldots, M_t)$, we can construct the piecewise linear functions as shown in Figure 5.
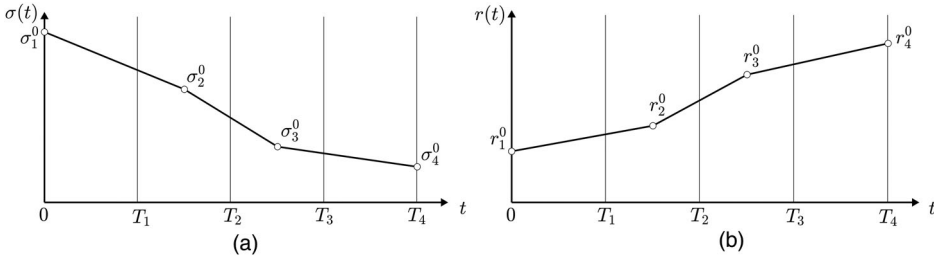
Figure 5. Schematic illustrations of the piecewise linear (a) volatility function and (b) interest rate function without exponentiation.
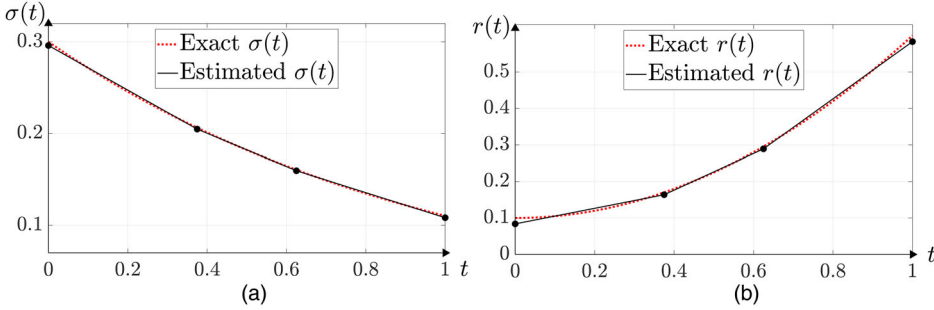

Figure 6. Estimated piecewise linear functions calibrated without exponentiation compared to (a) the exact volatility function $\sigma(t) = 0.3e^{-t}$ and (b) the exact interest rate function $r(t) = 0.5t^2 + 0.1$.

With these functions, we apply the calibration algorithm. Figure 6 represents the estimated piecewise linear functions. The MSE values are 1.1413e-6, 2.9398e-5 for volatility and interest rate, respectively.

We obtain almost the same result compared to the above test. However, there still probability that the estimated values may be negative in some cases. To prevent this problem, we include the step to take exponentiation.

3.2. Manufactured data 2

In this section, we consider another following non-linear manufactured volatility and interest rate functions:

$$\sigma(t) = 0.1\sin(4\pi t) - 0.1t + 0.2, \ r(t) = 0.15\cos(1.5\pi t) + 0.3t. \tag{7}$$

We obtained the best performed set $\{\sigma_n, r_n\}, n = 1, 2, \ldots, 6$ in the *lsqcurvefit* routine by solving Equation (3) with $T_\alpha = 30\alpha/360$ for $\alpha = 1, 2, \ldots, 12$ and $K_\beta = 70 + 10\beta$ for $\beta = 1, 2, \ldots, 5$.

Figure 7 represents the piecewise linear functions from the obtained set $\{\sigma_n, r_n\}, n = 1, 2, \ldots, 6$. Here, we use the same indications as above in Figure 3. Fluctuations of the two functions seem to be quite severe. We can gain very similar functions to the exact ones even in that case. In this case, the MSE values are 2.0756e-5, 9.5211e-7 for volatility and interest rate, respectively.

We conducted numerical experiments when large datasets with more maturities and strike prices are given and other optimization algorithms to demonstrate the robustness of the proposed algorithm. We consider the manufactured volatility and interest rate Equation (7) with $T_\alpha = 18\alpha/360$ for $\alpha = 1, 2, \ldots, 20$ and $K_\beta = 65 + 5\beta$ for $\beta = 1, 2, \ldots, 21$. The total market data is 420 prices.

Figure 8 represents the time-dependent functions from the obtained set $\{\sigma_n, r_n\}, n = 1, 2, \ldots, 20$. Here, we use the *lsqcurvefit* with the default trust-region-reflective algorithm. We can gain very similar
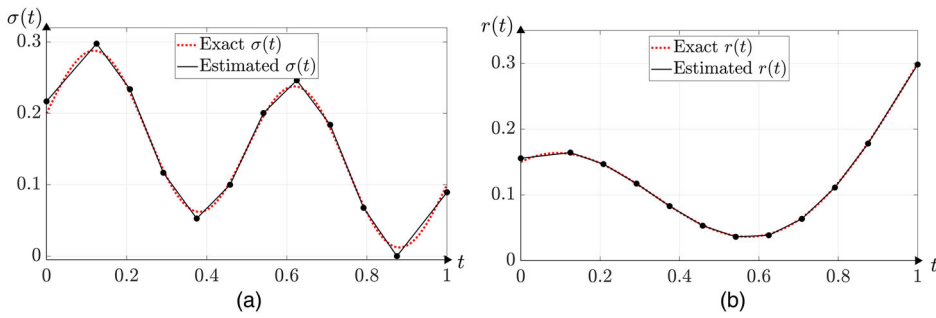
Figure 7. Estimated piecewise linear functions from the proposed algorithm compared to (a) the exact volatility function $\sigma(t) = 0.1\sin(4\pi t) - 0.1t + 0.2$ and (b) the exact interest rate function $r(t) = 0.15\cos(1.5\pi t) + 0.3t$.
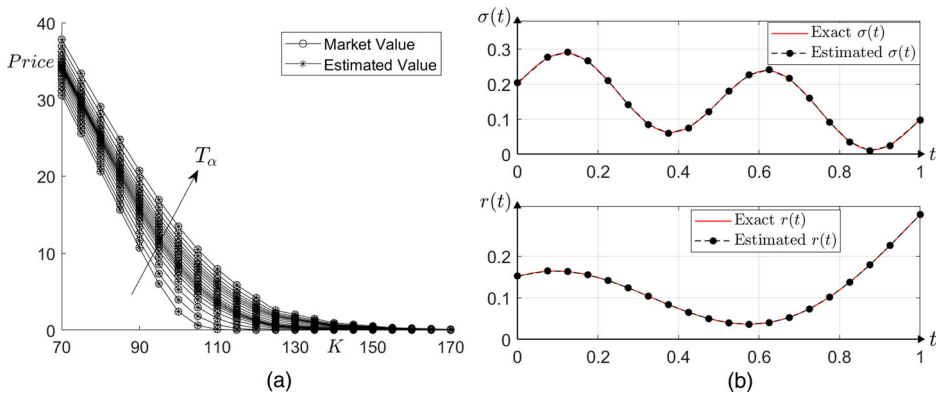

Figure 8. (a) Comparison of European call option price(circle-marked solid line) with numerical option prices (star-marked solid line). (b) Constructed volatility and interest rate function.

functions to the exact ones even in that case. In this case, the MSE values are 1.5245e-6, 0.0151 for volatility and interest rate, respectively.

Next, we looked at the performance for other optimization algorithms. For the previous test sets, we use the *lsqcurvefit* with the Levenberg–Marquardt algorithm to solve Equation (3).

Figure 9(a) shows the two algorithms converged to the same solution. In the Levenberg–Marquardt algorithm used, the MSE values are 1.5245e-6, 0.0151 for volatility and interest rate, respectively. The accuracy of the two algorithms is similar.

3.3. Stability test

In this section, we consider manufactured functions with white noise for stability. First, we construct new volatility and interest rate functions by adding white noise to the manufactured functions. The new noised functions are as follows:

$$\sigma_{\text{new}}(t) = \sigma(t)(1 + \gamma W_1),$$
$$r_{\text{new}}(t) = r(t)(1 + \gamma W_2),$$

where γ is a noise weight and W_1, W_2 follow standard normal distributions. Then, we apply our proposed algorithm using these functions. We conduct stability tests with functions (7). To recognize the effect of noise weight, we conduct tests in some cases. Figures 10 and 11 illustrate the obtained piecewise linear volatility and interest rate functions when $\gamma = 1/15, 1/5$. Here, the blue dots denote
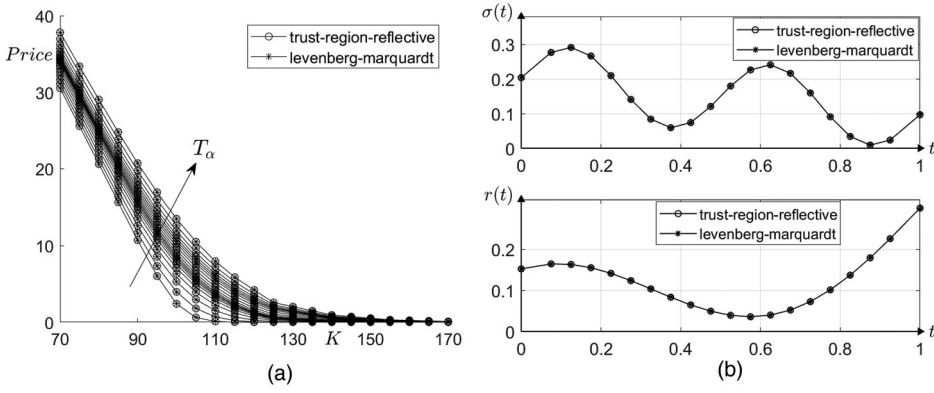
Figure 9. (a) Numerical option price, (b) Constructed volatility and interest rate function with the trust-region-reflective algorithm(circle-marked solid line) and the Levenberg–Marquardt algorithm(star-marked solid line).
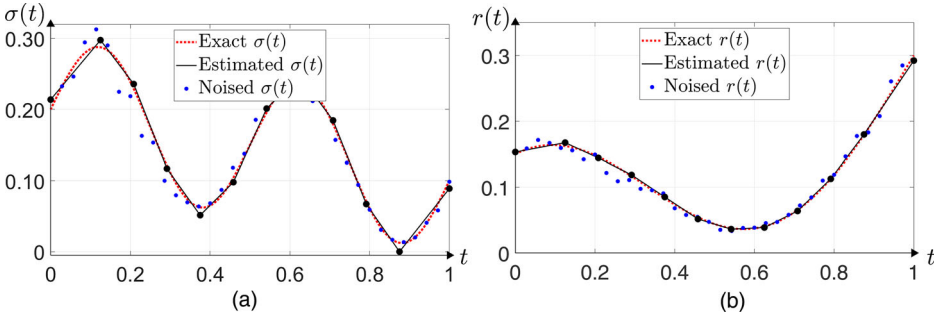

Figure 10. Estimated piecewise linear functions from the proposed algorithm with noise when $\gamma = \frac{1}{15}$ compared to (a) the exact volatility function $\sigma(t) = 0.1 \sin(4\pi t) - 0.1t + 0.2$ and (b) the exact interest rate function $r(t) = 0.15 \cos(1.5\pi t) + 0.3t$.

Figure 11. Estimated piecewise linear functions from the proposed algorithm with noise when $\gamma = \frac{1}{5}$ compared to (a) the exact volatility function $\sigma(t) = 0.1 \sin(4\pi t) - 0.1t + 0.2$ and (b) the exact interest rate function $r(t) = 0.15 \cos(1.5\pi t) + 0.3t$.
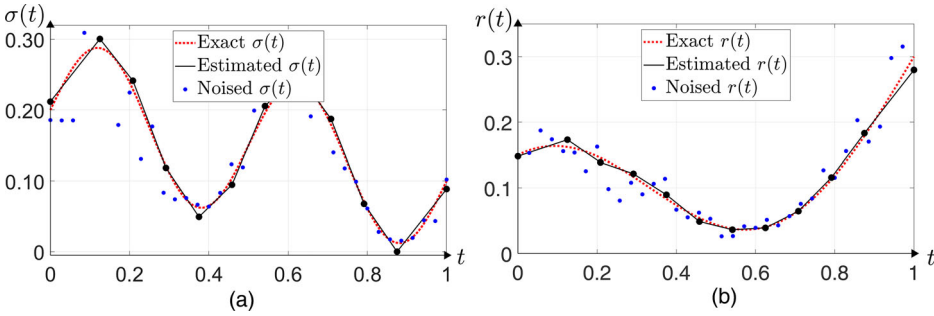
manufactured function with white noise. Table 2 shows the MSE values for volatility and interest rate in each case. Even in functions with noise, we can find that the proposed method exhibits stability.

3.4. Effective test

In this section, we demonstrate the effectiveness of the proposed method by performing the test in the paper [3]. We use the time-dependent volatility function in the test case1 of the paper [3]. The

Table 2. MSE values for manufactured volatility and interest rate functions with noise.

γ	1/5	1/10	1/15
σ	3.0483e−5	2.1917e−5	2.0925e−5
r	2.5853e−5	7.1310e−6	3.6782e−6
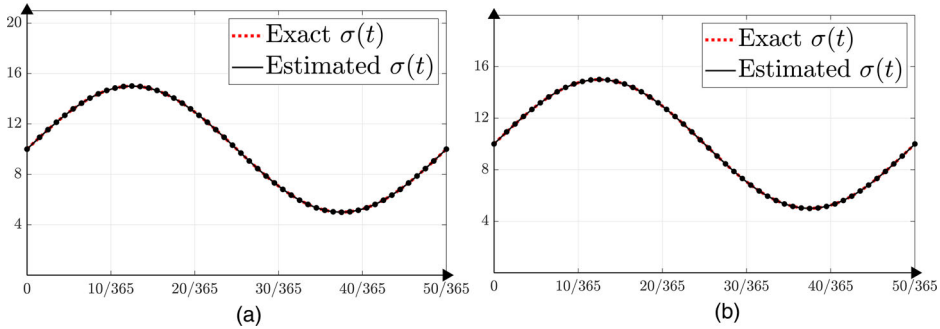
Figure 12. Exact time-dependent volatility function and Estimated time-dependent volatility function (a) call option and (b) put option.

time-dependent volatility function is followed:

$$\sigma(t) = 10 + 5 \sin\left(2\pi \frac{t}{T}\right), \quad 0 \le t \le T \tag{8}$$

The parameters used in this section are taken as follows: The underlying asset price S is chosen from 0 to 20 with asset price interval $\Delta S = 0.0625$, the initial underlying asset price $S_0 = 10$, time to maturity $T = 50/365$, time interval $\Delta t = 1/365$, the strike price $K = 11$, and interest rate $r = 0.2$. We are going to conduct two tests. We compute the call option price and the put option price using the parameters and the Levenberg–Marquardt algorithm. Then, we apply the proposed algorithm using the time-dependent volatility function (8). Here, the red dotted line denotes the exact time-dependent volatility function and the black solid line denotes the estimated time-dependent volatility function using the proposed method (Figure 12).

The average error for the exact and estimated functions is defined as

$$\text{Average error (\%)} = \frac{1}{N} \sum_{n=1}^{N} \left| \frac{\sigma_{n,\text{exact}} - \sigma_{n,\text{estimated}}}{\sigma_{n,\text{exact}}} \right| \times 100(\%). \tag{9}$$

In the reference paper [3], the average error for put option is observed with 2.47e−8%. Table 3 shows the average error for call and put option using the proposed algorithm. The proposed algorithm has been found to calibrate time-dependent volatility that is more similar to manufactured time-dependent volatility.

Table 3. Average error values for the exact time-dependent volatility and the estimated time-dependent volatility functions.

Option	Call	Put
Average error(%)	6.2652e−10	8.6030e−10

3.5. Manufactured data 3

On the third test, we consider manufactured volatility surface and constant interest rate:

$$\sigma(S,t) = \left(10^{-5}(S - S^*)^2 + 0.2\right)e^{-t}, \quad r(S,t) = 0.015, \tag{10}$$

where $S^* = 100$ and $S^* = 300$. Then $S^* = 100$ and $S^* = 300$ indicate 'smile' volatility and 'skew' volatility for the underlying asset, respectively (see Figure 13). We set $T_\alpha = 90\alpha/360$ for $\alpha = 1, 2, \ldots, 4$ and $K_\beta = 85 + 5\beta$ for $\beta = 1, 2, \ldots, 5$.

Figure 14(a ,b) show the estimated option price using the proposed algorithm for the manufactured volatility surface Equation (10) with $S^* = 100$ and (b) $S^* = 300$, respectively.

From Figure 14, we observe that we can construct the time-dependent volatility which covers the generated market prices using the manufactured volatility surface. However, because we propose the algorithm that constructs time-dependent volatility function, our model can not replicate the volatility smile and skew observed on the market in this paper. A local volatility surface of the underlying asset and time is left for future research.

3.6. Volatility and interest rate construction using KOSPI 200 data

Here, we conduct our proposed algorithm to get piecewise linear volatility and interest rate functions with KOSPI 200 index call option datasets on 30 December 2020. Table 4 indicates the real market data with respect to the strikes and maturities. Table 5 represents trading volume of the call option contract. Strikes used in these tables are $K_\beta = 395 + 2.5(\beta - 1)$ for $\beta = 1, 2, \ldots, 8$ and the maturity
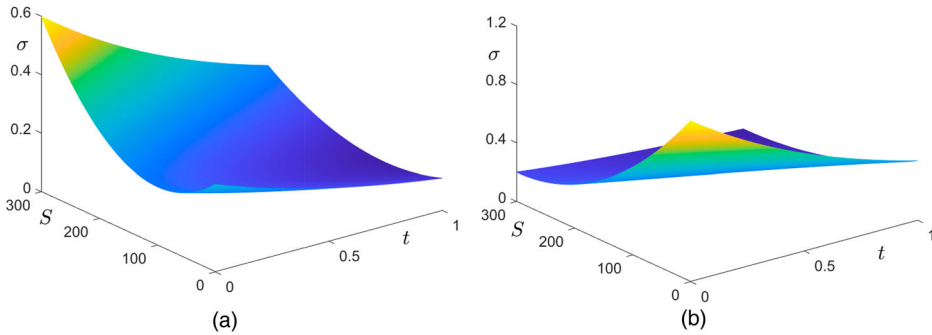

Figure 13. Manufactured volatility surface $\sigma(S,t) = (10^{-5}(S - S^*)^2 + 0.2)e^{-t}$ with (a) $S^* = 100$ and (b) $S^* = 300$.
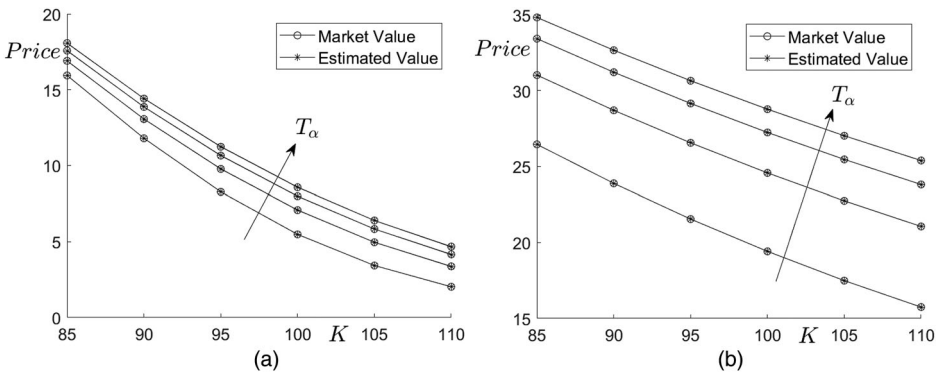

Figure 14. Estimated option price using the proposed algorithm for manufactured volatility surface $\sigma(S,t) = (10^{-5}(S - S^*)^2 + 0.2)e^{-t}$ with (a) $S^* = 100$ and (b) $S^* = 300$.

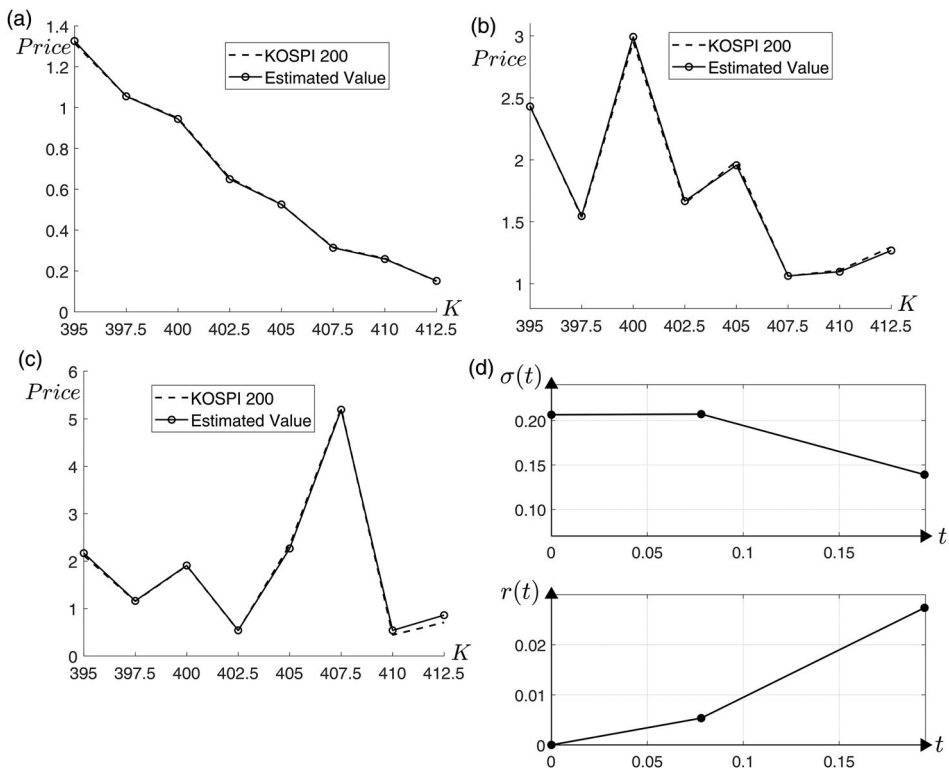**Table 4.** KOSPI 200 index call option price on 30 December 2020 with respect to the strike and maturity.

K_β	395.0	397.5	400.0	402.5	405.0	407.5	410	412.5
$T_1 = 15\Delta\tau$	3.70	2.95	2.31	1.79	1.35	1.02	0.76	0.54
$T_2 = 42\Delta\tau$	8.06	7.03	6.11	5.33	4.75	4.02	3.49	3.01
$T_3 = 71\Delta\tau$	10.25	9.40	8.48	7.56	7.03	6.10	4.42	3.91

Table 5. KOSPI 200 index call option volume on 30 December 2020 with respect to the strike and maturity.

K_β	395.0	397.5	400.0	402.5	405.0	407.5	410	412.5
$T_1 = 15\Delta\tau$	145957	148149	194886	155175	175479	110637	136867	88546
$T_2 = 42\Delta\tau$	512	268	1310	536	983	391	566	1041
$T_3 = 71\Delta\tau$	17	6	20	2	44	291	4	13

Table 6. Weighted KOSPI 200 index call option price on 30 December 2020 with respect to the strike and maturity.

K_β	395.0	397.5	400.0	402.5	405.0	407.5	410	412.5
$T_1 = 15\Delta\tau$	1.31	1.06	0.95	0.66	0.53	0.32	0.26	0.15
$T_2 = 42\Delta\tau$	2.44	1.54	2.95	1.65	1.99	1.06	1.11	1.30
$T_3 = 71\Delta\tau$	2.12	1.16	1.90	0.54	2.34	5.22	0.44	0.71

Figure 15. Comparison of weighted KOSPI 200 index call option price(dashed line) with numerical option prices (circle-marked solid line) at (a) $T = 15/365$, (b) $42/365$, and (c) $71/365$. (d) Constructed volatility and interest rate function.

times are $T_1 = 15\Delta\tau$, $T_2 = 42\Delta\tau$, and $T_3 = 71\Delta\tau$, where $\Delta\tau = 1/365$. At this time, the present value of the KOSPI 200 index was $S_0 = 389.29$. With Table 5, we can compute weighted market values with normalized weight from the trading volume. We can check that in Table 6.
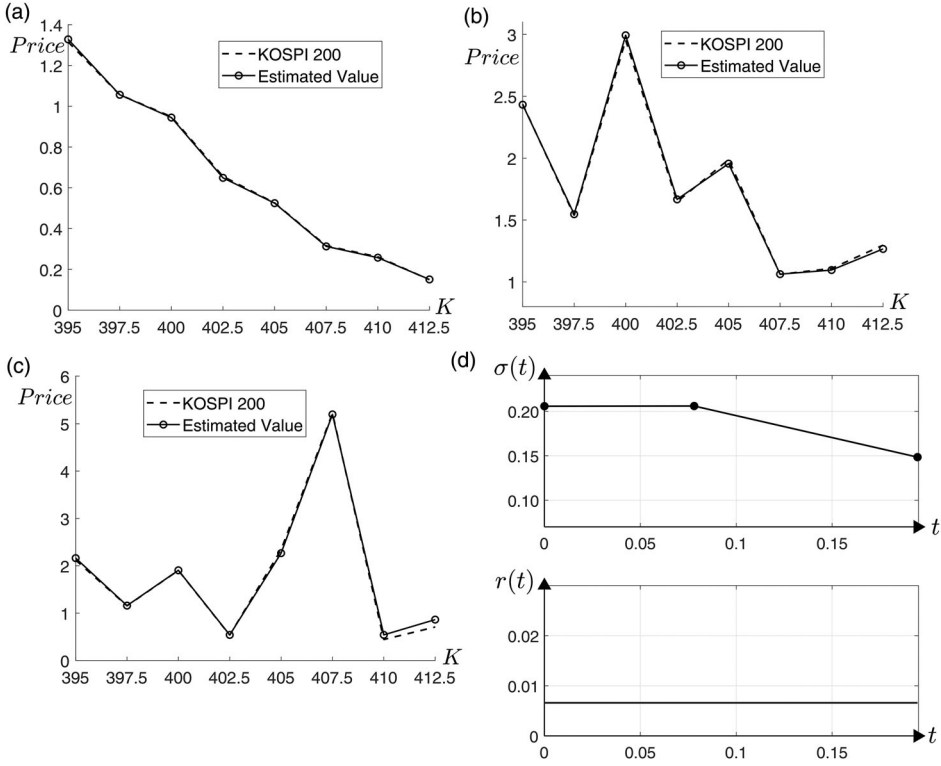
Figure 16. Comparison of weighted KOSPI 200 index call option price (dashed line) with numerical option prices (circle-marked solid line) at (a) $T = 15/365$, (b) $42/365$, and (c) $71/365$. (d) Constructed volatility and constant interest rate function.

We apply our calibration algorithm to this data with non-uniform spatial grid $\Omega = \{15i \mid i = 0, \dots, 25\} \cup \{S_0\} \cup \{390 + 1.25j \mid j = 0, \dots, 22\} \cup \{420 + 15k \mid k = 0, \dots, 49\}$. Figure 15 shows the result of our proposed algorithm. We can find that numerical values from our proposed algorithm are quite similar with the real market values at each maturity. It can be inferred from Figure 15(a–c). That is, our method also worked well in KOSPI 200 data. Additionally, we inserted the constructed volatility and interest rate function from the algorithm in Figure 15(d). It can be inferred from the tests conducted so far that the volatility and interest rate functions can be found well.

Also, we implement tests with consumption that the volatility or the interest rate is constant, respectively. The results are presented in Figures 16 and 17.

4. Conclusions

Many studies disclosed the assumption that volatility and interest rate are all constant values in the BS equation does not reflect well the real-world market. To overcome the vulnerability of the BS equation, we consider an algorithm that can construct the time-dependent volatility and interest rate function in this paper. The main goal of our paper is to find these two time-varying functions from the real market data. Because of the fact that volatility and interest rate are positive in the usual case, we use the exponential function to make the values obtained positive. Then, we can construct the piecewise linear structures of them by interpolating some points, which is obtained from the exponential function. When we construct the piecewise linear functions, we use the *lsqcurvefit*. As shown in Section 3, we demonstrate that our proposed algorithm works
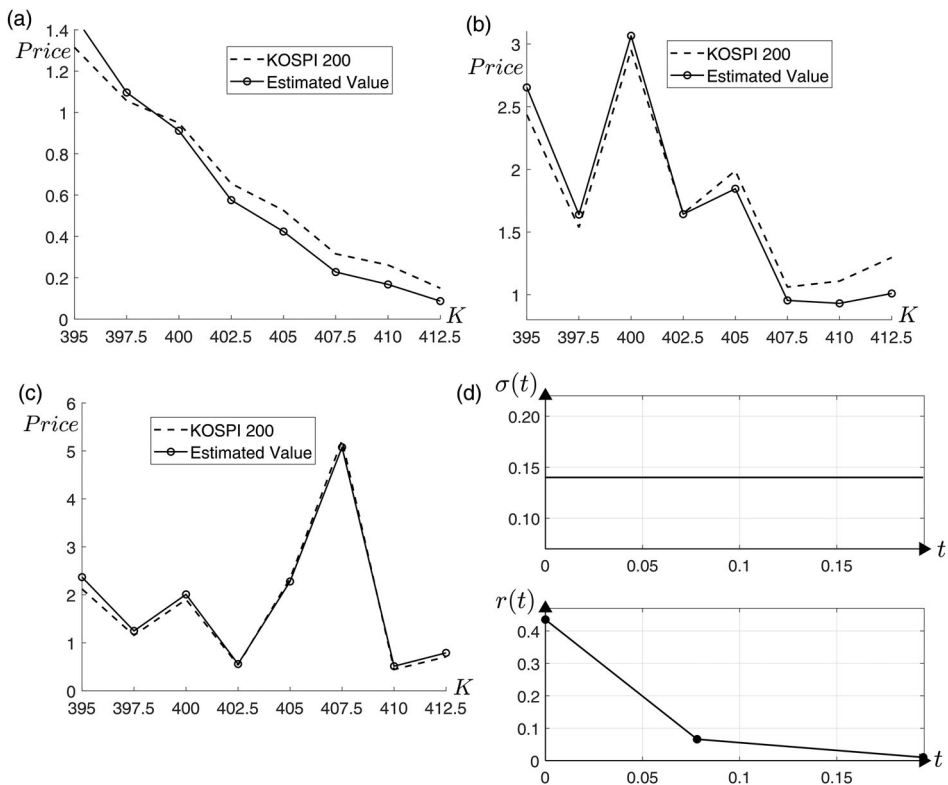
Figure 17. Comparison of weighted KOSPI 200 index call option price (dashed line) with numerical option prices (circle-marked solid line) at (a) $T = 15/365$, (b) 42/365, and (c) 71/365. (d) Constant volatility and constructed interest rate function.

well with obtained data from manufactured time-varying functions and the real market data, KOSPI 200.

Acknowledgments

Disclosure statement

ORCID

Junseok Kim http://orcid.org/0000-0002-0484-9189

References

[1] I. Arregui and J. Ráfales, *A stochastic local volatility technique for TARN options*, Int. J. Comput. Math. 97 (2020), pp. 1133–1149.
[2] F. Black and M. Scholes, *The pricing of options and corporate liabilities*, J. Polit. Econ. 81 (1973), pp. 637–654.
[3] H.M. Chen and C.H. Huang, *An inverse European option problem in estimating the time-dependent volatility function with statistical analysis*, Int. J. Syst. Sci. 36 (2005), pp. 103–111.
[4] J. Daněk and J. Pospíšil, *Numerical aspects of integration in semi-closed option pricing formulas for stochastic volatility jump diffusion models*, Int. J. Comput. Math. 97 (2020), pp. 1268–1292.

[5] A. Elettra and A. Rossella, *A generalization of the Geske formula for compound options*, Math. Soc. Sci. 45 (2013), pp. 75–82.

[6] L.A. Grzelak, *The collocating local volatility framework – a fresh look at efficient pricing with smile*, Int. J. Comput. Math. 96 (2019), pp. 2209–2228.

[7] L.A. Grzelak and C.W. Oosterlee, *On the Heston model with stochastic interest rates*, SIAM J. Financ. Math. 2 (2011), pp. 255–286.

[8] C. Guardasoni, *Semi-analytical method for the pricing of barrier options in case of time-dependent parameters (with matlab@@@ codes)*, Comun. Appl. Ind. Math. 9 (2018), pp. 42–67.

[9] X.J. He and W. Chen, *A closed-form pricing formula for European options under a new stochastic volatility model with a stochastic long-term mean*, Math. Financial Econ. 15 (2021), pp. 381–396.

[10] S.L. Heston, *A closed-form solution for options with stochastic volatility with applications to bond and currency options*, Rev. Financ. Stud. 6 (1993), pp. 327–343.

[11] F.A. Ko and R.J.A. David, *A numerical scheme for the Black–Scholes equation with variable interest rate using spectral collocation and backward-differences*, in Proceedings of the International MultiConference of Engineers and Computer Scientists 1, 2015, pp. 401–403.

[12] Y. Liang and C. Xu, *An efficient conditional Monte Carlo method for European option pricing with stochastic volatility and stochastic interest rate*, Int. J. Comput. Math. 97 (2020), pp. 638–655.

[13] S. Lin and X.J. He, *A closed-form pricing formula for forward start options under a regime-switching stochastic volatility model*, Chaos Solitons Fractals 144 (2021), pp. 110644.

[14] C.F. Lo and C.H. Hui, *Valuing double barrier options with time-dependent parameters by Fourier series expansion*, IAENG Int. J. Appl. Math. Comput. Sci. 36 (2007), pp. 1–5.

[15] The MathWorks Inc., *MATLAB*, Natick, MA, 1994, Software available at http://www.mathworks.com/.

[16] R.C Merton, *Theory of rational option pricing*, Int. J. Appl. Math. Comput. Sci. 4 (1973), pp. 141–183.

[17] R. Naz and I. Naeem, *Exact solutions of a Black–Scholes model with time-dependent parameters by utilizing potential symmetries*, Discret. Contin. Dyn. Syst.-Ser. S. 13 (2020), pp. 2841–2851.

[18] M.R. Rodrigo and R.S. Mamon, *An alternative approach to solving the Black–Scholes equation with time-varying parameters*, Appl. Math. Lett. 19 (2006), pp. 398–402.

[19] M.R. Rodrigo and R.S. Mamon, *An application of mellin transform techniques to a Black–Scholes equation problem*, Anal. Appl. 5 (2007), pp. 51–66.

[20] D. Tavella and C. Randall, *Pricing Financial Instruments: the Finite Difference Method*, Vol. 13, Jone Wiely and Sons, New York, 2000.

[21] L. Thomas, *Elliptic Problems in Linear Differential Equations Over a Network: Watson Scientific Computing Laboratory*, Columbia University, New York, 1949.

[22] H. Windcliff, P.A. Forsuth and K.R. Vetzal, *Analysis of the stability of the linear boundary condition for the Black–Scholes equation*, J. Comput. Financ. 8 (2004), pp. 65–92.

[23] S.H.I. Yunxia and Z.H.A.O. Xiping, *A novel method for prediction of option pricing for a market model*, Econ. Comput. Econ. Cybern. Stud. 47 (2013), pp. 1–14.